Arabian Journal of Chemistry (2023) **16**, 104588

King Saud University

Arabian Journal of Chemistry

www.ksu.edu.sa
www.sciencedirect.com

ORIGINAL ARTICLE

Design, synthesis, bioactivity and mechanism of action of novel myricetin derivatives containing amide and hydrazide

Xiao Cao, Fang Liu, Bangcan He, Li Xing, Yuanquan Zhang, Nian Zhang, Wei Xue *

State Key Laboratory Breeding Base of Green Pesticide and Agricultural Bioengineering; Key Laboratory of Green Pesticide and Agricultural Bioengineering, Ministry of Education; Research and Development Center for Fine Chemicals, Guizhou University, Guiyang 550025, PR China

Received 2 November 2022; accepted 11 January 2023
Available online 18 January 2023

KEYWORDS

Myricetin;
Amide;
Hydrazide;
Anti-TMV;
Insecticidal;
Mechanism

Abstract A series of myricetin derivatives containing amide and hydrazide were designed and synthesized. All the compounds were characterized by NMR and HRMS. Bioactivity test showed that some of the target compounds had excellent anti-tobacco mosaic virus (TMV) activity. In particular, the median effective concentration (EC_{50}) values of the anti-TMV curative and protective activities of *N*-(2-(2-(2-((5,7-dimethoxy-4-oxo-2-(3,4,5-trimethoxyphenyl)-4*H*-chromen-3-yl)oxy)acetyl) hydrazineyl)-2-oxoethyl)-4-(trifluoromethyl)benzamide (**G9**) were 202.3 and 164.0 μg/mL respectively, superior to ningnanmycin (329.1, 230.3 μg/mL). Microscale thermophoresis (MST) and molecular docking showed that **G9** had an excellent binding affinity with tobacco mosaic virus coat protein (TMV-CP) (K_d = 0.158 ± 0.024 μM), which was better than that of ningnanmycin (K_d = 2.074 ± 0.818 μM). Moreover, there were many interaction forces between **G9** and the key amino acid residues of TMV-CP. The chlorophyll content and peroxidase (POD) activity of tobacco leaves treated with **G9** increased significantly, indicating that **G9** could improve the photosynthesis of tobacco leaves and stimulate the resistance of tobacco leaves to TMV. The insecticidal activity of **G9** against *Mythimna separata* (*M. separate*) was found to be 95.2% at 200 μg/mL, which was close to bufenozide (100%). The insecticidal activity of myricetin was significantly improved after the introduction of active groups of amide and hydrazide, which could be further explored.

* Corresponding author.
E-mail address: wxue@gzu.edu.cn (W. Xue).

Peer review under responsibility of King Saud University.

Production and hosting by Elsevier

https://doi.org/10.1016/j.arabjc.2023.104588
1878-5352

Abbreviations used:

^{1}H NMR	^{1}H nuclear magnetic resonance
^{13}C NMR	^{13}C nuclear magnetic resonance
^{19}F NMR	^{19}F nuclear magnetic resonance
HRMS	High-resolution mass spectrometry
TMV	Tobacco mosaic virus
EC_{50}	Median effective concentration
MST	Microscale thermophoresis
TMV-CP	Tobacco mosaic virus coat protein
POD	peroxidase
M. separate	*Mythimna separate*
Xoo	*Xanthomonas oryzae pv oryzae*
Xac	*Xanthomonas axonopodis pv citri*
K_d	Binding constants
TLC	Thin layer chromatography
m.p.	Melting point
DMF	*N*,*N*-dimethylformamide
DMSO	Dimethylsulfoxide.

1. Introduction

Plant diseases and insect pests seriously restrict the normal growth and development of crops, which further cause the yield and quality of crops greatly reduced (Savary et al., 2019; Ren et al., 2020). TMV is known as "plant cancer". It has many hosts, wide transmission range and strong persistence (Lv et al., 2020). It can cause cell infection by directly contacting the injured position on the plant surface (Creager et al., 1999). The TMV is highly adaptable in the natural environment, and once infected, it is difficult for the plants to defend themselves through their own immune system. It has severely affected agricultural production, causing annual economic losses of up to $100 million worldwide (Bos, 2000). Therefore, the effective control of TMV still faces great challenge. At present, chemicals and synthetic compounds are still effective methods to control TMV infection in plants. However, the two most commonly used anti-plant virus agents, ningnanmycin and ribavirin, did not achieve satisfactory inhibitory effect due to their unsatisfactory field control effect and poor curative activity (Su et al., 2016; Gan et al., 2021; Yuan et al., 2022). Therefore, it is of great significance to develop new and practical antiviral drugs to control the virus.

Myricetin is a kind of flavonoids, which can be isolated from berries or tea, and is a natural product of plant origin (Pan et al., 2016; Ren et al., 2022). At present, myricetin has been reported to have antioxidant (Qiu et al., 2017), anti-tumor (Javed et al., 2022), bacteriostatic (Rashed et al., 2014), antiviral (Yu et al., 2012; Su et al, 2013) and other pharmacological effects. In addition, in previous studies by our group, it was found that myricetin has the effect of controlling plant diseases (Zhong et al., 2017). The research group modified the structure on the 3-hydroxyl group of myricetin, and obtained some myricetin derivative molecules with excellent bacteriostatic and anti-TMV biological activity by introducing some active groups, as shown in Fig. 1. Such as the introduction of piperidine sulfanilamide (Jiang et al., 2020a), dithiocarbamate (Jiang et al., 2020b), benzimidazole (Chen et al., 2021), etc., these drug molecules have excellent antibacterial activity *in vitro* against *Xanthomonas oryzae pv oryzae* (*Xoo*.) and *Xanthomonas axonopodis pv citri* (*Xac*.). Moreover, after the introduction of thiadiazol amide sulfide (Ruan et al., 2018), oxadiazole (Zhang et al., 2019), ferulic acid scaffolds (Tang et al., 2020), 1,3,4-oxadiazole sulfide (Peng et al., 2021), and quinazolinone (Liu et al., 2022) on the 3-hydroxyl group of myricetin, these drug molecules exhibited excellent *in vivo* anti-TMV activity. Based on this, myricetin as the lead compound can greatly enhance its biological activity after structural modification. This provides more ideas for the creation of new pesticides.

Amide is an important active fragment. Amide-containing compounds play an important role in bactericidal (Wu et al., 2021), insecticidal (Aguiar et al., 2019), herbicide (Wang et al., 2009) and antiviral drugs (Luo et al., 2020). The bishydrazide group contains two formamides, and compounds containing bishydrazide also exhibit a variety of good biological activities, such as insecticidal activity (Li et al., 2019), antibacterial (Zhou et al., 2020; Li et al., 2022) and anti-tumor (Sun et al., 2014), etc.

In this study, a series of myricetin derivatives containing amide and hydrazide were designed and synthesized by introducing the structure containing amide into myricetin by hydrazide bypass. The design idea of the target compounds is shown in Fig. 2. Based on the excellent anti-TMV activity of myricetin, we continue to do research in this area. In addition, we also evaluated the insecticidal activity of the prepared myricetin derivatives, which was unprecedented in our group's previ-

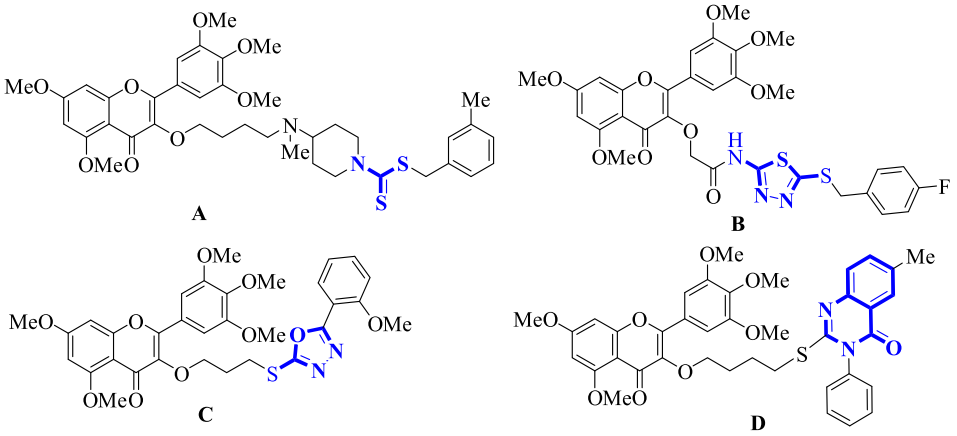

Fig. 1 Myricetin derivatives with excellent biological activity.

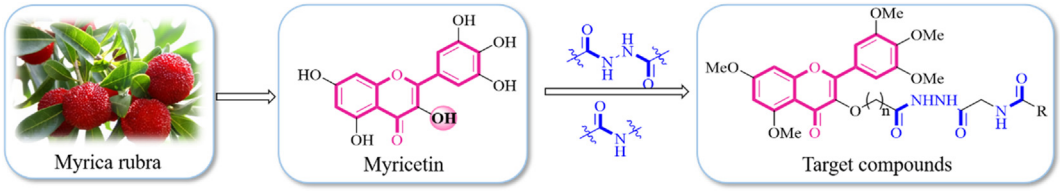

Fig. 2 Design idea for target compounds.

ous research. Then, the mechanism of action of the compounds with excellent activity was preliminarily investigated by MST, molecular docking, chlorophyll and defense enzyme content determination.

2. Materials and methods

2.1. Instruments and chemicals

The target compounds **G1-G22** were characterized by nuclear magnetic resonance spectrometer with deuterium dimethyl sulfoxide as solvent (Bruker, Germany) and Thermo scientific Q Executive mass spectrometer (Missour, USA). The melting point data were measured by X-4B melting point instrument (Shanghai INESA Co., Ltd.) without calibration. The binding constants (K_d) values of compounds to TMV-CP were determined by using NanoTemp Monolith NT.115 microscale thermophoresis (NanoTemper, Germany). All reagents used are analytical pure without further purification. All acyl chloride compounds used were purchased from Shanghai tansoole platform. The peroxidase kit was purchased from Suzhou Keming Biotechnology Co., Ltd. (Jiangsu, China).

2.2. Synthesis

*2.2.1. General synthesis procedure of **intermediates 1–1** to **1–4***

A previous method was used made by us to prepare **intermediates 1–1** to **1–4** (Mokale et al., 2014; Xue et al., 2015), and slightly modified **intermediate 1–2**. **Intermediate 1–1** (1.5 mmol), *N*,*N*-dimethylformamide (DMF) (15 mL) and K_2CO_3 (2.25 mmol) were added into a three neck round bottom flask, stirred at room temperature for 15 min, and then added ethyl bromide carboxylate. The reaction was monitored with thin layer chromatography (TLC) for about 2.5 h at 60 °C. After the reaction stopped, ice water was poured and vacuum filtered.

*2.2.2. General synthesis procedure of target compounds **G1-G22***

The synthesis process of the target compounds **G1-G22** was shown in Scheme 1, which was obtained from the literature (Wang et al., 2019). At room temperature, the **intermediate 1–4** (1.2 mmol), *O*-(benzotriazol-1-yl)-*N*,*N*,*N*',*N*'-tetramethyluroniumtetrafluoroborate (TBTU) (1.2 mmol) and NEt_3 (3.6 mmol) were stirred in 15 mL of dichloromethane for 30 min. The **intermediate 1–3** (1 mmol) dissolved in dichloromethane was added to the obtained solution and stirred overnight. Vacuum filtered the white sediment and washed it with dichloromethane to obtain the target compounds.

2.3. Biological assays

2.3.1. Antiviral activity

Three modes *in vivo* (curative, protective and inactivating activity) of compounds anti-TMV were identified by methods described in the literature (Song et al., 2005; Guo et al., 2020). Myricetin and commercial antiviral agent ningnanmycin were used as positive controls.

2.3.2. Insecticidal activity

The insecticidal activity was determined by leaf soaking method (Li et al., 2020; Jiang et al., 2020), and the commercial drug tebufenozide and dimethylsulfoxide (DMSO) were used as positive control and blank control. The target compounds

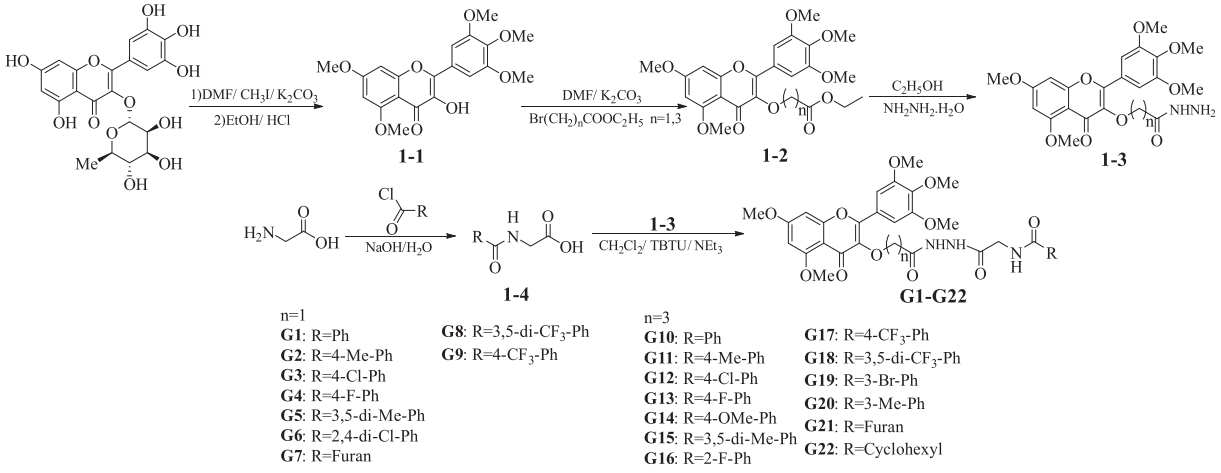

Scheme 1 Synthetic route of target compounds **G1**−**G22**.

and tebufenozide were dissolved in DMSO and diluted to a concentration of 200 μg/mL with tween 80 containing 0.1%. Fresh maize leaves grown in the greenhouse were cut into shapes of the same size and soaked in the liquid medicine for 0.5 min. Then, 15 second-instar *M. separate* of the same size were randomly selected and placed on the treated leaves. All samples were placed in an artificial climate chamber with 25 °C, 80% humidity, 14 h of light and 10 h of darkness. And lasted for 72 h.

The corrected mortality was calculated by the formula:

$$I(\%) = (T - C) \times 100/(100\% - C)$$

"I" is the corrected mortality, "*T*" is the mortality of the drug group, and "*C*" is the mortality of the blank group (*T* and *C* are expressed as percentages).

2.4. Microscale thermophoresis

According to the MST test method reported in the literature (Chen et al., 2019; Zhou et al., 2018), the binding affinity of **G9** and **G13** to TMV-CP were measured. The ningnanmycin and the lead compound myricetin were tested as the positive control.

2.5. Molecular docking

The molecular docking of myricetin, **G9**, and ningnanmycin with TMV-CP were achieved according to the previously reported method (Chen et al., 2019). TMV-CP (PDB ID: 1EI7) was obtained from the Protein Database (PDB, https://www.rcsb.org) as a template for molecular docking. Molecular docking and visual analysis were performed by Discovery Studio and Pymol software.

2.6. The content of chlorophyll

The contents of chlorophyll *a*, chlorophyll *b* and total chlorophyll in tobacco leaves were measured according to the method reported in the literature (Fan et al., 2011; Gan et al., 2017; Liu et al., 2022).

2.7. The activity of peroxidase

According to the method previously reported (Fan et al., 2011; Gan et al., 2017; Liu et al., 2022), the POD content in tobacco leaves was measured with an enzyme assay kit.

3. Result and discussion

3.1. Chemistry

As can be seen from Scheme 1, the target compounds **G1-G22** were prepared by de-glycolysis, etherification, hydrazation, substitution and condensation reaction. The ^{1}H NMR, ^{13}C NMR, ^{19}F NMR and HRMS spectral data of the target compounds were offered in the Appendix A. Supplementary materia.

3.2. Anti-TMV activity in vivo

The anti-TMV activities of the target compounds **G1-G22** at 500 μg/mL *in vivo* were evaluated by the half leaf spot method. The data of antiviral activities of the target compounds are shown in Table 1. Most of the target compounds showed excellent anti-TMV activity. **G9, G12, G13, G14** and **G17** showed good curative effects anti-TMV with values of 64.8, 59.2, 61.5, 58.7 and 59.7%, respectively, which were superior to ningnanmycin (58.3%). In addition, **G9**, **G13** and **G14** also had significant protective effects anti-TMV with values of 71.3, 69.5 and 69.4% respectively, which were higher than the ningnanmycin (67.5%). *In vivo* leaf diagram of **G9** and ningnanmycin anti-TMV is shown in Fig. 3.

In order to more accurately determine the compounds with better primary screening activity, their EC_{50} values were further tested, as shown in Table 2. The EC_{50} values of antiviral curative activity of **G9** (202.3 μg/mg), **G12** (209.7 μg/mg), **G13** (297.3 μg/mg), **G14** (317.0 μg/mg) and **G17** (274.4 μg/mg) were superior to those of ningnanmycin (329.1 μg/mg). The EC_{50} value of antiviral protective activity of **G9** (164.0 μg/mg), **G13** (211.7 μg/mg), and **G14** (218.7 μg/mg) were better than those of ningnanmycin (230.3 μg/mg). From their structures, we were surprised to find that the substituents of these compounds are all in the para position of the benzene ring.

3.3. Structure–activity relationships (SARs)

Combined with the activity data in Table 1 and Table 2, the structures of some compounds with better activity share some common characteristics. Antiviral data showed that **G9** (4-CF_3-Ph, 202.3 μg/mg), **G12** (4-Cl-Ph, 209.7 μg/mg), **G13** (4-F-Ph, 297.3 μg/mg) and **G17** (4-CF_3-Ph, 274.4 μg/mg) showed outstanding curative activity anti-TMV, superior to **G14** (4-OMe-Ph, 317.0 μg/mg). **G9** (4-CF_3-Ph, 164.0 μg/mg) and **G13** (4-F-Ph, 211.7 μg/mg) showed better protective activity anti-TMV, superior to **G14** (4-OMe-Ph, 218.7 μg/mg). The structural formulas of compounds **G9** and **G14** are shown in Fig. 4. When there is an electron-absorbing group in the para-position of the benzene ring, the antiviral activity is better than that of the electron-donor group, indicating that the para-electron-absorbing group of the benzene ring is conducive to improving its antiviral activity.

3.4. The results of MST

The binding affinity of the compound to TMV-CP can be evaluated by the K_d value. The interactions between **G9**, **G13**, myricetin and ningnanmycin with TMV-CP were analyzed by MST studies. As can be seen from Fig. 5 and Table 3, the binding ability of **G9** (0.158 ± 0.024 μM) and TMV-CP was stronger than that of **G13** (0.201 ± 0.109 μM), while the binding ability of myricetin (71.220 ± 33.686 μM) and ningnanmycin (2.074 ± 0.818 μM) to TMV-CP were much weaker than those of **G9**, **G13**. MST results were consistent with antiviral activity. These results indicated that the excellent anti-TMV activity of **G9** is due to its strong binding ability to TMV-CP.

Table 1 *In vivo* anti-TMV activity of target compounds.[a]

Compd.	n	R	Curation	Protection	Inactivation
G1	1	Ph	51.1 ± 1.2	63.8 ± 5.8	64.7 ± 2.5
G2	1	4-Me-Ph	50.5 ± 5.6	60.5 ± 4.1	45.0 ± 3.8
G3	1	4-Cl-Ph	56.7 ± 6.2	60.7 ± 3.9	54.7 ± 7.0
G4	1	4-F-Ph	54.6 ± 1.9	57.3 ± 3.6	54.8 ± 1.9
G5	1	3,5-di-Me-Ph	51.3 ± 2.4	63.7 ± 9.5	56.0 ± 4.5
G6	1	2,4-di-Cl-Ph	50.5 ± 3.1	46.5 ± 7.4	41.0 ± 0.8
G7	1	Furan	55.1 ± 4.9	59.5 ± 5.6	45.2 ± 3.0
G8	1	3,5-di-CF_3-Ph	45.7 ± 5.7	54.5 ± 1.3	48.9 ± 3.2
G9	1	4-CF_3-Ph	64.8 ± 3.3	71.3 ± 2.0	74.2 ± 1.5
G10	3	Ph	53.9 ± 1.5	65.4 ± 4.4	49.2 ± 4.4
G11	3	4-Me-Ph	57.0 ± 7.0	61.5 ± 4.6	64.0 ± 2.4
G12	3	4-Cl-Ph	59.2 ± 1.9	56.9 ± 3.9	68.2 ± 3.4
G13	3	4-F-Ph	61.5 ± 5.1	69.5 ± 2.1	61.7 ± 7.8
G14	3	4-OMe-Ph	58.7 ± 8.6	69.4 ± 4.5	46.7 ± 3.0
G15	3	3,5-di-Me-Ph	56.0 ± 5.7	55.3 ± 4.6	54.4 ± 4.0
G16	3	2-F-Ph	48.6 ± 4.8	58.3 ± 6.1	52.8 ± 1.3
G17	3	4-CF_3-Ph	59.7 ± 0.7	65.8 ± 1.6	68.7 ± 4.6
G18	3	3,5-di-CF_3-Ph	51.5 ± 2.7	61.8 ± 5.7	52.7 ± 5.5
G19	3	3-Br-Ph	49.5 ± 3.3	53.6 ± 4.4	57.1 ± 6.7
G20	3	3-Me-Ph	49.6 ± 3.6	52.9 ± 2.8	61.2 ± 3.4
G21	3	Furan	51.3 ± 3.0	55.8 ± 7.0	30.4 ± 3.1
G22	3	Cyclohexyl	54.1 ± 7.7	51.9 ± 3.7	53.8 ± 4.9
myricetin [b]			45.6 ± 4.9	47.3 ± 1.6	48.4 ± 4.4
ningnanmycin [c]			58.3 ± 3.5	67.5 ± 3.6	94.8 ± 2.4

[a] Average values of three repeated experiments; [b] The control myricetin; [C] The control drug ningnanmycin.

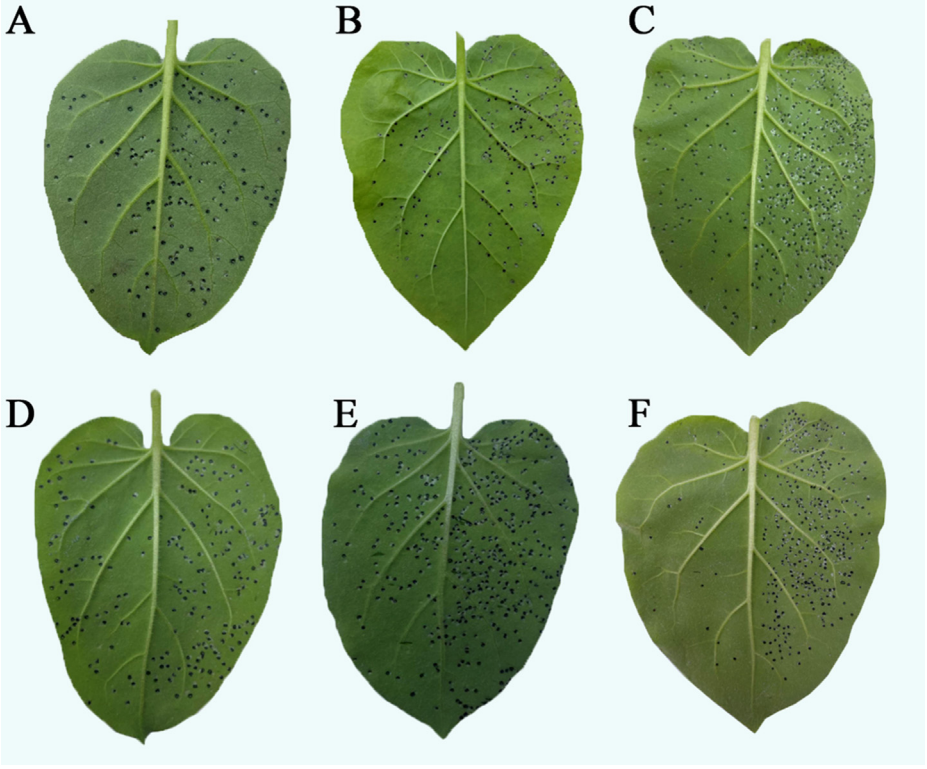

Fig. 3 Morphological effects of **G9** and ningnanmycin on TMV. **G9** (A. Curation, B. Protection, C. Inactivation); ningnanmycin (D. Curation, E. Protection, F. Inactivation) (Left lobe: drug treated; Right lobe: blank control).

Table 2 EC_{50} of TMV with some target compounds.

	Compd.	Regression equation	r	EC_{50}(μg/mL)
Curative activity	**G9**	y = 0.8297x + 3.0868	0.9755	202.3 ± 2.2
	G12	y = 0.7366x + 3.2822	0.9843	209.7 ± 3.3
	G13	y = 0.8359x + 2.9327	0.9986	297.3 ± 3.9
	G14	y = 0.9067x + 2.7323	0.9961	317.0 ± 3.9
	G17	y = 0.8415x + 2.9481	0.9964	274.4 ± 4.3
	ningnanmycin	y = 0.9046x + 2.7228	0.9877	329.1 ± 3.2
Protective activity	**G9**	y = 0.9290x + 2.9279	0.9869	164.0 ± 2.9
	G13	y = 1.1715x + 2.2755	0.9903	211.7 ± 2.0
	G14	y = 1.3280x + 1.8936	0.9947	218.7 ± 2.1
	ningnanmycin	y = 1.2083x + 2.1456	0.9834	230.3 ± 3.7

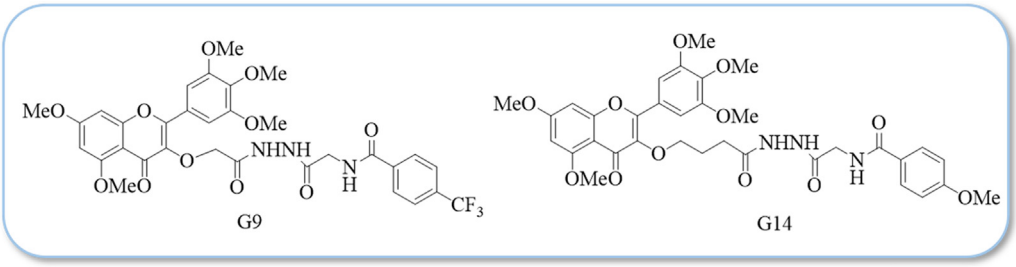

Fig. 4 The structural formulas of compounds **G9** and **G14**.

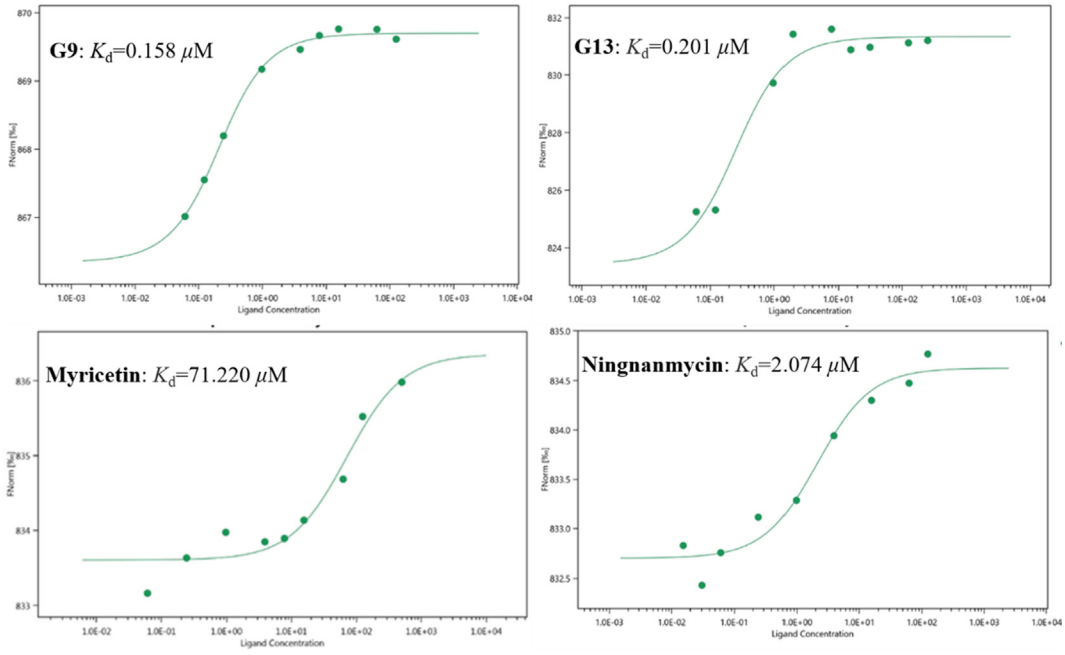

Fig. 5 The MST results of **G9**, **G13**, myricetin and ningnanmycin to TMV-CP.

3.5. Molecular docking

The results of MST study showed that **G9** had excellent binding affinity with TMV-CP. Therefore, molecular docking of myricetin, **G9** and ningnanmycin were carried out to explore the similarities and differences in their binding modes.

Fig. 6 shows that myricetin, **G9** and ningnanmycin were well embedded in the active pocket of TMV-CP. From the docking results, it could be seen that there are many identical amino acid residues among the three. The common amino acid residues between **myricetin**, **G9** and TMV-CP are ASN73, ARG134, TYR139 and VAL260. The same amino acid residues between **G9**, ningnanmycin and TMV-CP are ASN73, GLU131, ARG134, SER138, TYR139, PRO254 and LYS268. Fig. 6 **B** and **C** also show that **G9** and ningnanmycin were connected to the active pocket of TMV-CP in a similar

Table 3 The K_d of compounds to TMV-CP.

Compd.	K_d value (μM)
G9	0.158 ± 0.024
G13	0.201 ± 0.109
myricetin	71.220 ± 33.628
ningnanmycin	2.074 ± 0.818

posture. This may also be a factor in the good anti-TMV activity of **G9** (Wang et al., 2021).

In addition, myricetin interacts with amino acid residue ARG134 through three conventional hydrogen bonds. There were eight traditional hydrogen bonds between **G9** and TMV-CP, among which formamide and "-CF_3" on the hydrazide fragment interact firmly with amino acid residues SER255 and SER143 through two traditional hydrogen bonds (2.46 Å, 2.17 Å) and hydrogen bonds (2.81 Å), respectively. There were six hydrogen bonds between ningnanmycin and TMV-CP, which was lower than that of **G9**. In addition, **G9** binds well to PHE67 and TYR139 through Pi-Pi T-shaped and Pi-Alkyl, respectively. Relevant studies have shown that such amino acid residues have good hydrophobicity and play a key role in the self-assembly of TMV-CP (Bloomer et al., 1978; Luo et al., 2020). The above molecular docking results provided a strong indication that **G9** has excellent antiviral activity.

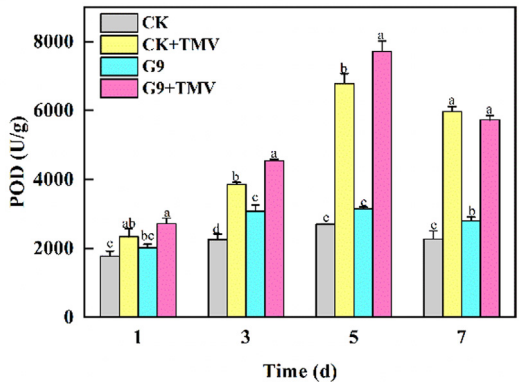

Fig. 8 Changes of POD activity in tobacco leaves treated with **G9**.

3.6. Determination of chlorophyll content

The content of chlorophyll directly affects the health of plants, and chlorophyll plays a decisive role in plant photosynthesis. As shown in Fig. 7, the chlorophyll content in the body of the susceptible group infected with TMV gradually decreased with the passage of time. In contrast, the chlorophyll content of leaves treated with **G9** increased most significantly on the 5th day, and reached the highest value (1.125 mg/g) on the 5th day. In the healthy group without TMV infection, the

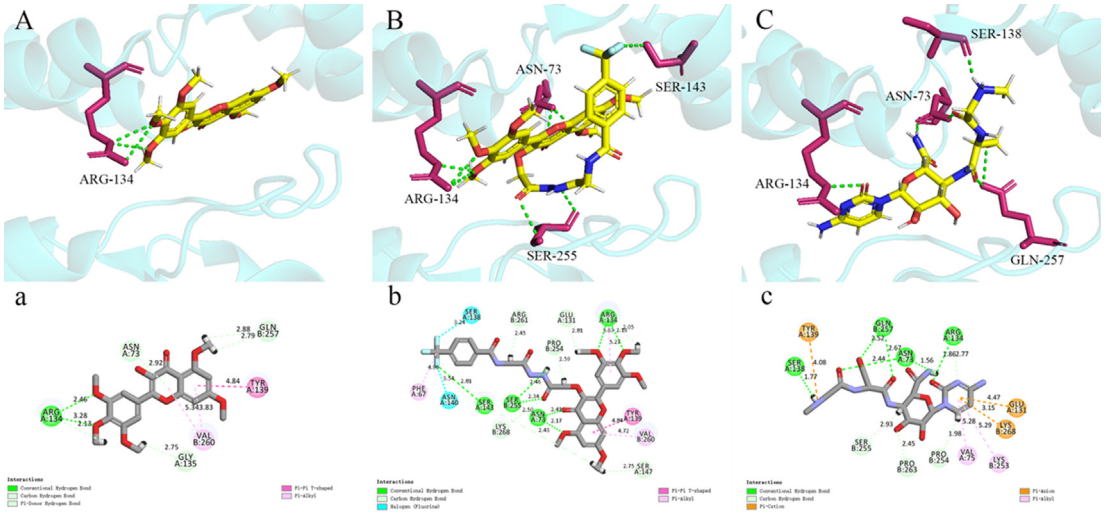

Fig. 6 Molecular docking of myricetin, **G9** and ningnanmycin to TMV-CP. myricetin (A, a), **G9** (B, b), ningnanmycin (C, c).

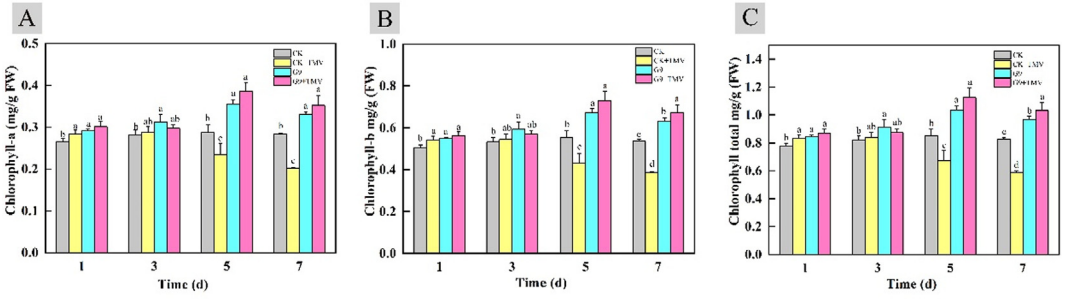

Fig. 7 Changes of chlorophyll content in tobacco leaves treated with **G9**. (A: Chlorophyll *a*; B: Chlorophyll *b*; C: the total chlorophyll).

Table 4 Insecticidal activity of the target compounds.

Compd.	R	Mortality (%) (200 μg/mL)	Compd.	R	Mortality (%) (200 μg/mL)
G1	Ph	22.3	**G13**	4-F-Ph	57.5
G2	4-Me-Ph	35.1	**G14**	4-OMe-Ph	4.8
G3	4-Cl-Ph	58.2	**G15**	3,5-di-Me-Ph	33.9
G4	4-F-Ph	21.0	**G16**	2-F-Ph	6.0
G5	3,5-di-Me-Ph	71.7	**G17**	4-CF_3-Ph	43.3
G6	2,4-di-Cl-Ph	38.4	**G18**	3,5-di-CF_3-Ph	46.9
G7	Furan	7.7	**G19**	3-Br-Ph	32.4
G8	3,5-di-CF_3-Ph	77.7	**G20**	3-Me-Ph	30.2
G9	4-CF_3-Ph	95.2	**G21**	Furan	13.5
G10	Ph	35.9	**G22**	Cyclohexyl	6.1
G11	4-Me-Ph	37.1	myricetin		3.9
G12	4-Cl-Ph	41.0	Teb.[a]		100.0

[a] The Commercial drug tebufenozide.

chlorophyll content in leaves was basically unchanged from the first day to the seventh day. However, after treatment with **G9**, there was a relatively obvious improvement. The maximum value was 1.037 mg/g on the fifth day. These results indicated that **G9** treatment could improve the anti-TMV defense ability of tobacco leaves, and then improve the photosynthetic capacity of tobacco leaves.

3.7. Determination of POD activity

The changes of POD activity in tobacco leaves are shown in Fig. 8. In the susceptible group infected with TMV, POD activity in tobacco leaves increased from the first day to the fifth day, and reached the peak on the fifth day. In the healthy group without TMV infection, POD activity increased slowly, but after treatment with **G9**, POD activity in tobacco leaves was relatively increased. The results showed that **G9** could promote the increase of POD activity in tobacco leaves and improve disease resistance of tobacco.

3.8. Insecticidal activity

According to the structure of the designed target compounds, *M. separate* was selected as the experimental object. The insecticidal activities of the target compounds are shown in Table 4. Most of the compounds showed some insecticidal activity at a concentration of 200 μg/mg. **G9** had the best insecticidal activity with a mortality of 95.2%, which was slightly lower than that of bufenozide (100%). Myricetin showed negligible insecticidal activity compared with **G9** and bufenozide. It can be seen from this result that the insecticidal ability of myricetin was significantly improved by introducing our active group into the structure of myricetin.

4. Conclusion

In summary, a series of myricetin derivatives containing amide and hydrazine were designed in an attempt to develop potential antiviral agents and insecticides. The antiviral bioassay results showed that the EC_{50} values of the anti-TMV curative activities of some compounds were 202.3 (**G9**), 209.7 (**G12**), 297.3 (**G13**), 317.0 (**G14**) and 274.4 μg/mL (**G17**). The EC_{50} values of protective activity were 164.0 (**G9**), 211.7 (**G13**) and 218.7 μg/mL (**G14**). The results of MST and molecular docking showed that **G9** and TMV-CP exhibited excellent binding affinity and multiple interaction forces. The chlorophyll content and POD activity of tobacco leaves treated with **G9** increased significantly, indicating that **G9** could improve the photosynthesis of tobacco leaves and stimulate the resistance of tobacco leaves to TMV. In addition, insecticidal activity was screened and it was found that the mortality of **G9** against *M. separate* was close to that of bufenozide at 200 μg/mL. The insecticidal activity of myricetin was significantly improved after the introduction of amide and hydrazide, which could be further studied.

Declaration of Competing Interest

The authors declare that they have no known competing financial interests or personal relationships that could have appeared to influence the work reported in this paper.

Acknowledgements

This research was completed with the support of the National Natural Science Foundation of China (No. 21867003), the Science Foundation of Guizhou Province (No. 20192452), Key Laboratory of Institute of Environment and Plant Protection (No. HZSKFKT202208).

Appendix A. Supplementary material

Information on the structural characterization of the target compounds can be found online at https://doi.org/10.1016/j.arabjc.2023.104588.

References

Aguiar, A.R., Alvarenga, E.S., Silva, E.M., et al, 2019. Synthesis, insecticidal activity, and phytotoxicity of novel chiral amide. Pest Manag. Sci. 75, 1689–1696.

Bloomer, A.C., Champness, J.N., Bricogne, G., et al, 1978. Protein disk of tobacco mosaic virus at 2.8 Å resolution showing the interactions within and between subunits. Nature 276, 362–368.

Bos, L., 2000. 100 years of virology: from vitalism via molecular biology to genetic engineering. Trends Microbiol. 8, 82–87.

Chen, L.J., Wang, X.B., Tang, X., et al, 2019. Design, synthesis, antiviral bioactivities and interaction mechanisms of penta-1,4-diene-3-one oxime ether derivatives containing a quinazolin-4(3*H*)-one scaffold. BMC Chem. 13, 34.

Chen, M., Tang, X.M., Liu, T.T., et al, 2021. Antimicrobial evaluation of myricetin derivatives containing benzimidazole skeleton against plant pathogens. Fitoterapia 149, 104804.

Chen, Y., Li, P., Su, S.J., et al, 2019. Synthesis and antibacterial and antiviral activities of myricetin derivatives containing a 1,2,4-triazole Schiff base. RSC Adv. 9, 23045–23052.

Creager, A.N., Scholthof, K.B., Citovsky, V., et al, 1999. Tobacco mosaic virus. Pioneering research for a century. Plant Cell 11, 301–308.

Fan, H.T., Song, B.A., Bhadury, P.S., et al, 2011. Antiviral activity and mechanism of action of novel thiourea containing chiral phosphonate on tobacco mosaic virus. Int. J. Mol. Sci. 12, 4522–4535.

Gan, X.H., Wang, Z.X., Hu, D.Y., 2021. Synthesis of Novel Antiviral Ferulic Acid-Eugenol and Isoeugenol Hybrids Using Various Link Reactions. J. Agric. Food Chem. 69, 13724–13733.

Gan, X.H., Hu, D.Y., Wang, Y.J., et al, 2017. Novel trans-Ferulic Acid Derivatives Containing a Chalcone Moiety as Potential Activator for Plant Resistance Induction. J. Agric. Food Chem. 65, 4367–4377.

Guo, T., Xia, R.J., Liu, T.T., et al, 2020. Synthesis, Biological Activity and Action Mechanism Study of Novel Chalcone Derivatives Containing Malonate. Chem. Biodivers. 17, e2000025.

Javed, Z., Khan, K., Jesús, H.B., et al, 2022. Myricetin: targeting signaling networks in cancer and its implication in chemotherapy. Cancer Cell Int. 22, 239.

Jiang, B.B., Jin, X.Y., Dong, Y.W., et al, 2020. Design, Synthesis, and Biological Activity of Novel Heptacyclic Pyrazolamide Derivatives: A New Candidate of Dual-Target Insect Growth Regulators. J. Agric. Food Chem. 68, 6347–6354.

Jiang, S.C., Tang, X., Chen, M., et al, 2020. Design, synthesis and antibacterial activities against *Xanthomonas oryzae pv. oryzae*, *Xanthomonas axonopodis pv. Citri* and *Ralstonia solanacearum* of novel myricetin derivatives containing sulfonamide moiety. Pest Manag. Sci. 76, 853–860.

Jiang, S.C., Su, S.J., Chen, M., et al, 2020. Antibacterial Activities of Novel Dithiocarbamate-Containing 4*H*-Chromen-4-one Derivatives. J. Agric. Food Chem. 68, 5641–5647.

Li, F.Y., Liu, J.B., Gong, J.N., et al, 2019. (R)-2-Phenyl-4,5-Dihydrothiazole-4-Carboxamide Derivatives Containing a Diacylhydrazine Group: Synthesis, Biological Evaluation, and SARs. Molecules 24, 4440.

Li, H.D., Wu, S., Yang, X., et al, 2022. Synthesis, Antibacterial Activity, and Mechanisms of Novel Indole Derivatives Containing Pyridinium Moieties. J. Agric. Food Chem. 70, 12341–12354.

Li, Q.Q., Wu, Z.M., Zhang, M., et al, 2020. Synthesis and Preliminary Exploration of Biological Activity of 3-Aryl-4-arylamine Methyl Isoxazoles. Chin. J. Org. Chem. 40, 2108–2113.

Liu, T.T., Peng, F., Zhu, Y.Y., et al, 2022. Design, synthesis, biological activity evaluation and mechanism of action of myricetin derivatives containing thioether quinazolinone. Arab. J. Chem. 15, 104019.

Luo, D.X., Guo, S.X., He, F., et al, 2020. Design, Synthesis, and Bioactivity of alpha-Ketoamide Derivatives Bearing a Vanillin Skeleton for Crop Diseases. J. Agric. Food Chem. 68, 7226–7234.

Lv, X., Xiang, S.Y., Wang, X.C., et al, 2020. Synthetic chloroinconazide compound exhibits highly efficient antiviral activity against tobacco mosaic virus. Pest Manag. Sci. 76, 3636–3648.

Mokale, S.N., Lokwani, D.K., Shinde, D.B., 2014. Synthesis, in-vitro reverse transcriptase inhibitory activity and docking study of some new imidazol-5-one analogs. Med. Chem. Res. 23, 3752–3764.

Pan, H.L., Hu, Q., Wang, J.Y., et al, 2016. Myricetin is a novel inhibitor of human inosine 5'-monophosphate dehydrogenase with anti-leukemia activity. Biochem. Biophys. Res. Commun. 477, 915–922.

Peng, F., Liu, T.T., Wang, Q.F., et al, 2021. Antibacterial and Antiviral Activities of 1,3,4-Oxadiazole Thioether 4*H*-Chromen-4-one Derivatives. J. Agric. Food Chem. 69, 11085–11094.

Qiu, S.S., Jiang, C.C., Yao, H., et al, 2017. Theoretical Investigation on the Relationship between the Structures and Antioxidant Activities of Myricetin and Dihydromyricetin. Chin. J. Struc. Chem. 36, 416–422.

Rashed, K., Ćirić, A., Glamočlija, J., et al, 2014. Antibacterial and antifungal activities of methanol extract and phenolic compounds from Diospyros virginiana L. Ind. Crop. Produ. 59, 210–215.

Ren, Q., Zhao, S.Y., Zhu, Y.J., et al, 2022. Supramolecular aggregates of myricetin improve its bioavailability and its role in counteracting alcoholism. J. Drug. Deliv. Sci. Tec. 74, 103515.

Ren, X.L., Li, X.Y., Yin, L.M., et al, 2020. Design, Synthesis, Antiviral Bioactivity, and Mechanism of the Ferulic Acid Ester-Containing Sulfonamide Moiety. ACS Omega 5, 19721–19726.

Ruan, X.H., Zhang, C., Jiang, S.C., et al, 2018. Design, Synthesis, and Biological Activity of Novel Myricetin Derivatives Containing Amide, Thioether, and 1,3,4-Thiadiazole Moieties. Molecules 23, 3132.

Savary, S., Willocquet, L., Pethybridge, S.J., et al, 2019. The global burden of pathogens and pests on major food crops. Nat. Ecol. Evol. 3, 430–439.

Song, B.A., Zhang, H.P., Wang, H., et al, 2005. Synthesis and Antiviral Activity of Novel Chiral Cyanoacrylate Derivatives. J. Agric. Food Chem. 53, 7886–7891.

Su, B., Cai, C.L., Deng, M., et al, 2016. Spatial Configuration and Three-Dimensional Conformation Directed Design, Synthesis, Antiviral Activity, and Structure-Activity Relationships of Phenanthroindolizidine Analogues. J. Agric. Food Chem. 64, 2039–2045.

Su, X.W., D'Souza, D.H., 2013. Naturally occurring flavonoids against human norovirus surrogates. Food Environ. Virol. 5, 97–102.

Sun, J., Lv, P.C., Guo, F.J., et al, 2014. Aromatic diacylhydrazine derivatives as a new class of polo-like kinase 1 (PLK1) inhibitors. Eur. J. Med. Chem. 81, 420–426.

Tang, X., Zhang, C., Chen, M., et al, 2020. Synthesis and antiviral activity of novel myricetin derivatives containing ferulic acid amide scaffolds. New J. Chem. 44, 2374–2379.

Wang, B.L., Ma, Y., Li, Y.H., et al, 2009. The design, synthesis of amide KARI inhibitors and their biological activities. Front. Chem. Chin. 4, 186–190.

Wang, X.B., Fu, X.C., Chen, M., et al, 2019. Novel 1,3,5-thiadiazine-2-thione derivatives containing a hydrazide moiety: Design, synthesis and bioactive evaluation against phytopathogenic fungi *in vitro* and *in vivo*. Chin. Chem. Lett. 30, 1419–1422.

Wang, X.B., Wang, M.Q., Han, L., et al, 2021. Novel Pyrazole-4-acetohydrazide Derivatives Potentially Targeting Fungal Succinate Dehydrogenase: Design, Synthesis, Three-Dimensional Quantitative Structure-Activity Relationship, and Molecular Docking. J. Agric. Food Chem. 69, 9557–9570.

Wu, Z.B., Shi, J., Chen, J.X., et al, 2021. Design, Synthesis, Antibacterial Activity, and Mechanisms of Novel 1,3,4-Thiadiazole Derivatives Containing an Amide Moiety. J. Agric. Food Chem. 69, 8660–8670.

Xue, W., Song, B.A., Zhao, H.J., et al, 2015. Novel myricetin derivatives: Design, synthesis and anticancer activity. Eur. J. Med. Chem. 97, 155–163.

Yu, M.S., Lee, J., Lee, J.M., et al, 2012. Identification of myricetin and scutellarein as novel chemical inhibitors of the SARS coronavirus helicase, nsP13. Bioorg. Med. Chem. Lett. 22, 4049–4054.

Yuan, T., Wang, Z.X., Lan, S.C., et al, 2022. Design, synthesis, antiviral activity, and mechanisms of novel ferulic acid derivatives containing amide moiety. Bioorg. Chem. 128, 106054.

Zhang, C., Jiang, S.C., Chen, Y., et al, 2019. Synthesis and Biological of Novel Myricetin Derivatives Containing 1,3,4-Oxadiazoles. Chin. J. Org. Chem. 39, 1160–2116.

Zhong, X.M., Wang, X.B., Chen, L.J., et al, 2017. Synthesis and biological activity of myricetin derivatives containing 1,3,4-thiadiazole scaffold. Chem. Cent. J. 11, 106.

Zhou, D.G., Xie, D.D., He, F.C., et al, 2018. Antiviral properties and interaction of novel chalcone derivatives containing a purine and benzenesulfonamide moiety. Bioorg. Med. Chem. Lett. 28, 2091–2097.

Zhou, X., Feng, Y.M., Qi, P.Y., et al, 2020. Synthesis and Docking Study of *N*-(Cinnamoyl)-*N*'-(substituted)acryloyl Hydrazide Derivatives Containing Pyridinium Moieties as a Novel Class of Filamentous Temperature-Sensitive Protein Z Inhibitors against the Intractable *Xanthomonas oryzae pv. oryzae* Infections in Rice. J. Agric. Food Chem. 68, 8132–8142.